

 Open access • Journal Article • DOI:10.1039/C4MH00124A

Sublattice-induced symmetry breaking and band-gap formation in graphene

— [Source link](#) 

Ralph Skomski, Peter A. Dowben, M. Sky Driver, Jeffery A Kelber





Institutions: University of Nebraska–Lincoln, University of North Texas

Published on: 06 Oct 2014 - Materials horizons (The Royal Society of Chemistry)

Topics: Direct and indirect band gaps, Explicit symmetry breaking, Band gap, Symmetry breaking and Symmetry (physics)

Related papers:

- [Generalized Gradient Approximation Made Simple](#)
- [The rise of graphene](#)
- [The electronic properties of graphene](#)
- [Substrate-induced band gap in graphene on hexagonal boron nitride: Ab initio density functional calculations](#)
- [Electric Field Effect in Atomically Thin Carbon Films](#)

Share this paper:    

View more about this paper here: <https://typeset.io/papers/sublattice-induced-symmetry-breaking-and-band-gap-formation-0466z29pcx>

2014

Sublattice-induced symmetry breaking and bandgap formation in graphene

Ralph A. Skomski

University of Nebraska-Lincoln, rskomski2@unl.edu

Peter A. Dowben

University of Nebraska-Lincoln, pdowben@unl.edu

M Sky Driver

University of North Texas

Jeffery A. Kelber

University of North Texas

Follow this and additional works at: <http://digitalcommons.unl.edu/physicsdowben>



Part of the [Physics Commons](#)

Skomski, Ralph A.; Dowben, Peter A.; Driver, M Sky; and Kelber, Jeffery A., "Sublattice-induced symmetry breaking and bandgap formation in graphene" (2014). *Peter Dowben Publications*. 262.

<http://digitalcommons.unl.edu/physicsdowben/262>

This Article is brought to you for free and open access by the Research Papers in Physics and Astronomy at DigitalCommons@University of Nebraska - Lincoln. It has been accepted for inclusion in Peter Dowben Publications by an authorized administrator of DigitalCommons@University of Nebraska - Lincoln.

CrossMark
click for updatesCite this: *Mater. Horiz.*, 2014, 1, 563Received 14th July 2014
Accepted 26th August 2014

DOI: 10.1039/c4mh00124a

rsc.li/materials-horizons

Sublattice-induced symmetry breaking and band-gap formation in graphene

Ralph Skomski,^a P. A. Dowben,^{*a} M. Sky Driver^b and Jeffry A. Kelber^b

A reduction of symmetry from C_{6v} to C_{3v} leads to the opening of a band gap in the otherwise gapless semiconductor graphene. Simple models provide a fairly complete picture of this mechanism for opening a band gap and in fact can be discussed in terms of the tight-binding approximation, accurately resolving the wave-vector space to a very high accuracy. This picture is consistent with experiments that yield a band gap due to A and B graphene-site symmetry breaking due to substrate interactions.

A. Introduction

There are various widely publicized approaches to engineering a band gap in graphene, such as strain engineering,^{1–4} spatial restriction, for example *via* graphene nanoribbon fabrication,^{5–16} controlling the density of electrons as in adsorbate hybridization,^{17–21} and symmetry breaking,^{22–41} typically as a result of substrate interactions. All have major flaws when the goal is retention of the unique properties of graphene while opening a band gap.

The creation of a band gap with *strain* has been investigated both theoretically^{1–3,42–44} and experimentally.^{44–47} Theoretical models are pretty consistent in showing that a band gap will open in graphene for some types of uniaxial strain but not for isotropic (affine) strain.^{1–4} The effective mass (m_{eff}) for uniaxially strained graphene, which is really the key parameter, in addition to the band gap, has sadly not been realistically considered in many of the model calculations of the strain-induced graphene band gap, with only a few exceptions.⁴ It is the large increase in m_{eff} that diminishes the value of opening a band gap in graphene, as this increase is usually considerable.⁴ For graphene nanoribbons the situation is worse: not only is there a huge increase in effective mass, but edge scattering will be significant, further diminishing an already lack-luster carrier mobility.^{11,48–51} Recent transport measurements,⁵² for graphene nanoribbons of 40 nm width, width have shown impressive mobilities, of 10^5 to 10^7 $\text{cm}^2 \text{V}^{-1} \text{s}^{-1}$. This suggests that edge

^aDepartment of Physics and Astronomy, The Nebraska Center for Materials and Nanoscience, University of Nebraska-Lincoln, Jorgensen Hall, 855 North 16th Street, Lincoln, NE 68588-0229, USA. E-mail: pdowben1@unl.edu

^bDepartment of Chemistry, Center for Electronic Materials Processing and Integration, University of North Texas, Denton, TX 76203, USA



Ralph Skomski is a Research Full Professor at the University of Nebraska (UNL). He is a polymer physicist by education then switched to magnetism as his main research area. He received his PhD from the Technical University Dresden, followed by post-doctoral positions at Trinity College Dublin and Max-Planck Institute Halle. Ralph Skomski is a Fellow of the American Physical Society and

widely known for his theoretical work in permanent magnetism and analytical magnetic modeling, with two authoritative books in these fields. He has pioneered the understanding of three-dimensional magnetic nanocomposites and is an expert in magnetic-anisotropy and crystal-field theory.



Peter Dowben is a Charles Bessey Professor of Physics at the University of Nebraska (UNL). He received this PhD from the University of Cambridge followed by a post-doctoral position at the Fritz Haber Institute. He is a Fellow of the American Physical Society, a Fellow of the Institute of Physics and a Fellow of the American Vacuum Society. Peter Dowben has pioneered resonant photoemission as a

means of investigating metallicity, pioneered angle resolved XPS for the study of boundary segregation and contributed to advances in molecular magneto-electrics along with providing additional demonstrations of boundary magnetization in magneto-electrics.

scatter may not always be a dominant factors for some graphene nanoribbon widths, but these nanoribbons were grown on SiC, where heavy n-doping is likely^{26,40,47,53,54} and a band gap with the chemical potential placed mid gap is unlikely. This leaves adsorbate or substrate induced band gaps as a more promising avenue for band gap engineering of graphene.

When considering a substrate induced modification of the gapless graphene, a band gap of zero²² to 0.16 eV (ref. 23) has been predicted for the single layer graphene between boron nitride layers while a band gap of 0.35 eV was predicted for graphene placed epitaxial registry on SiO₂,²⁴ generally larger band gaps in graphene than the band gap of about 53 meV predicted for graphene on BN²⁵ resulting from symmetry breaking. Obviously charge disorder or breaking of the A and B site symmetry matters.

A band gap of 0.26 eV has been experimentally determined for graphene on SiC,^{28,40} attributed to A and B site symmetry breaking, but is not a true band gap as the graphene is heavy n-type doped and the chemical potential (Fermi level) does not fall in the gap. Not just substrate symmetry breaking, but Bernal stacking, and the charge gradient due to substrate interactions, are expected to open a band gap for a trilayer graphene on SiC,⁵⁵ but again, this is not a true band gap as the graphene is heavy n-type doped and the chemical potential (Fermi level) does not fall in the gap. Scanning tunneling microscopy spectroscopy finds a 100 meV gap, at zero bias,⁵⁶ suggesting Fermi level placement midgap. In fact, both experimental band mapping and the scanning tunneling microscopy results for graphene on SiC may not be indicative of a band gap at all. Similar band structure mappings,^{53,54} attributed the distortions in the band structure near the Dirac point to electron-plasmon scattering^{41,53,57,58} and lateral scattering,^{53,59} not a direct result of A and B site symmetry breaking.

An even larger band gap approximately 0.5–1 eV, is found for graphene on MgO, where again the band gap is believed to be a result of symmetry breaking^{29–31} in the graphene. This band gap

for graphene on MgO, of order of 1/2 eV in experiment,^{31,32} is found to be larger than predicted by theory.^{33,34} Importantly, a band gap of about 180 meV has been predicted for graphene on the Al-terminated Al₂O₃(0001) surface, with an increase in electron effective mass of about $8 \times 10^{-3} m_e$.³⁵ Experimental studies of graphene grown directly on Al₂O₃(0001), however, revealed no evidence of a room temperature band gap.⁶⁰ Thus theory does not always predict a smaller band gap than observed in experiment.

Other extrinsic breaking of symmetry is also possible. For Bernal-stacked bilayer graphene, carriers occupy the non-stacked sites of the two layers equally, in the absence of a perpendicular electric field, leading to the degeneracy of the conduction and valence bands at the charge neutrality (Dirac) point.⁶¹ As with the predictions applied to graphene on SiC,^{41,54,55} the application of a perpendicular electric field opens a band gap up to 0.25 eV and renders the transport insulating.^{36–39,41} For single layer graphene between boron nitride layers, application of an electric field also leads to an increased band gap in the range of 0.23 eV (ref. 22) to 0.34 eV.²³

In some sense, almost all approaches to opening a band gap in graphene also result in symmetry breaking, but all schemes involving sublattice modification seem to involve this mechanism. Our goal here is to provide an overall explanation of the effect, based on the chemical inequivalence of the A and B sites of graphene: breaking the AB sublattice symmetry of the graphene and reducing the symmetry from C_{6v} to C_{3v} .

B. Graphene on h-BN(0001)

Density functional theory calculations for isolated graphene/BN bilayers,²⁵ indicated that the most stable configuration for graphene on BN places the C atoms above N atoms and the center of BN rings (Fig. 1). Such a configuration manifestly breaks the chemical equivalence of graphene A and B lattice sites, resulting in a predicted band gap of 0.053 eV (53 meV).²⁵ Consistent with



M. Sky Driver received his BS degree in physics and applied mathematics from the University of Idaho in 2006. He continued his studies at the University of Missouri – Kansas City; completing his MS and PhD in physics in 2009 and 2013, respectively. He is currently working as a Postdoctoral Research Associate at the University of North Texas in the Department of Chemistry,

studying the surface/interface interactions of novel electronic and spintronic materials. His research interests include the direct growth graphene and h-BN, and the development of novel or emerging electronic materials, including boron carbide-based polymers for neutron voltaic applications.



Jeffrey Kelber is a Regents Professor of Chemistry at the University of North Texas (UNT). He received his PhD in Inorganic Chemistry from the University of Illinois at Champaign-Urbana. He has received three inventor-recognition awards from the Semiconductor Research Corporation and the Dougherty Award from the Texas Division of the American Chemical Society. His group as

focused on the development of emerging electronic materials, including the direct growth of graphene on dielectric substrates, and the development of boron carbide/aromatic composite systems.

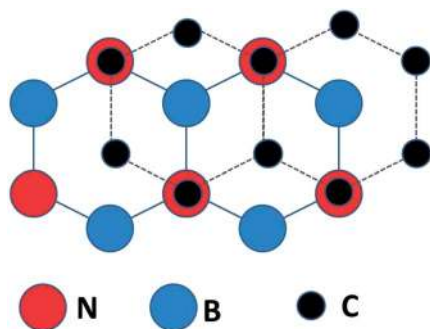


Fig. 1 The C sites are alternatively directly over N sites or the centers of the B–N ring in the calculated lowest energy configuration for an isolated graphene/BN(0001) bilayer (after ref. 25).

other theory,²⁵ changing the on-site potential difference between the carbon atoms in graphene, and the boron and nitrogen atoms in the h-BN, has been predicted to increase the induced gap,²⁷ if the graphene is in registry with the boron nitride.

Experimental formation of graphene/BN bilayers has involved a number of approaches including physical transfer of graphene to BN crystallites,^{62–64} and direct growth by CVD of graphene on BN deposited by atomic layer deposition (ALD).^{65,66} Studies involving physically transferred graphene generally have not investigated the relative orientation of the bilayers, and revealed no evidence of a band gap in the graphene.⁴⁶ For graphene not precisely in registry with the hexagonal boron nitride, the expectation is that a gap may be induced at the graphene “Dirac point” while a new superlattice of Dirac points develop at finite energy,²⁶ yet such graphene overlayers exhibit very high mobilities of $25\,000\text{ cm}^2\text{ V}^{-1}\text{ s}^{-1}$ (ref. 62) to $37\,000\text{ cm}^2\text{ V}^{-1}\text{ s}^{-1}$ (ref. 67) and above, consistent with little or no band gap.

Graphene/BN bilayers with graphene and BN in registry with each other can be formed by direct growth on transition metal substrates. Typically the BN moiety consists of a monolayer resulting from self-limiting pyrolysis of borazine or similar precursors.^{67–79} However, graphene has been directly grown on BN(0001) nanoflakes by various methods.^{80,81} Graphene/BN bilayers formed by direct growth on Ni(111) (ref. 65) or Ru(0001) (ref. 65) do indicate that the graphene and BN sheets are in registry with each other, consistent with Fig. 1 and expectations,²⁵ although the precise relative coordination of the two layers was not determined from the reported LEED data.

The metallic substrate can influence the BN electronic structure. This is manifest from a close inspection of the data in Fig. 2. The photoemission/inverse photoemission data (Fig. 2a) indicate no observable band gap at room temperature. This is consistent with the STM dI/dV data for the graphene/BN/Ru(0001) heterojunction (Fig. 2b) and the BN/Ru(0001) heterojunction prior to graphene growth (Fig. 2c). The scanning tunneling microscopy (STM) dI/dV data indicate significant Ru hybridization in valence and conduction bands of the BN monolayer (Fig. 2c): the BN monolayer, for example, exhibits a band gap of $\sim 2\text{ eV}$ compared to the 5.97 eV gap of bulk h-BN(0001).^{30,65}

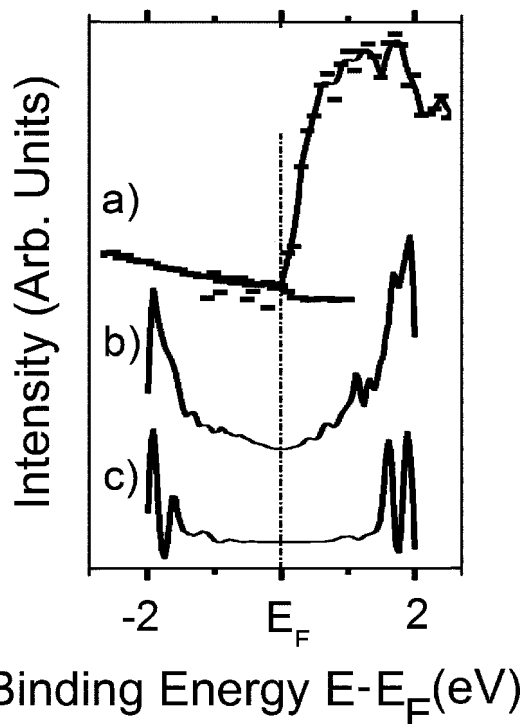


Fig. 2 The experimental density of states data for graphene/h-BN/Ru(0001) obtained from the combined PES and ARIPES data (a) and; (b) the STM dI/dV data (b). For comparison the STM dI/dV data for h-BN/Ru(0001) is also shown (c). All binding energies are referenced to the Fermi level as $E - E_F$. From ref. 65.

Consistent with the very small predicted band gap of 0.053 eV (53 meV) for graphene on boron nitride, the combined photoemission/inverse photoemission data (Fig. 2a) and the STM dI/dV data (Fig. 2b) show no evidence of a band gap in the (room temperature) density of states for graphene/h-BN/Ru(0001),³⁰ but again substrate effects are difficult to completely exclude. The direct growth of graphene on multilayer BN may be expected to diminish the effects of the metal substrate interactions with the first BN overlayer, and afford a clearer understanding of graphene/BN interactions and large-area h-BN(0001) multilayers have been fabricated by atomic layer deposition.⁸²

Misalignment of the graphene with a substrate, even a substrate like h-BN, can result from the graphene placement with respect to the substrate lattice. For graphene not grown in registry with the h-BN lattice, a Moiré pattern results as the crystallographic directions of the graphene rotated with respect to the substrate. In terms of electronic structure, this causes a folding of the graphene band structure in momentum space, potentially resulting in the replication of multiple Dirac points at symmetric densities away from the zero energy Dirac point.^{83–87} Worse yet, graphene bilayers, misaligned from one another might well result in something akin to a 2 dimensional electron gas.⁸⁸ These misaligned graphene to h-BN or graphene to graphene bilayers represent weak van der Waals interactions, but strong interactions are also *deleterious* to formation of any band gap, such as introduced by a partial transition metal layer

in close proximity to graphene,^{89,90} which leads to a density of states at the Fermi level.

C. Graphene on MgO(111)

It is not enough to simply open a band gap in graphene, as shown with graphene on SiC,^{28,40,91} as noted above, the chemical potential need not fall midgap as adsorbates or substrate interactions may also dope the graphene. More promising in this regard has been graphene on oxides (although not Al₂O₃ (ref. 60)) but where with the correct surface termination or oxide surface reconstruction, the graphene is no longer a gapless semiconductor, but an insulator.^{31,32,34,35} The low energy electron diffraction (LEED) data, in Fig. 3, indicates that graphene growth on the reconstructed surface of MgO(111) leads to a 1 monolayer (ML) graphene film that is actually of C_{3v} symmetry rather than six-fold symmetry (Fig. 3a).^{29,30,32} This indicates that in the first layer, the chemical equivalence of the graphene A sites and B sites has been lifted, apparently due to interactions with the MgO substrate. This pattern of 3-fold symmetry is also observed for few-layer graphene on MgO(111),^{29,30,32} as seen in Fig. 3b. The formation of an oxidized carbon component coinciding with the onset of long-range order and a C_{3v} LEED pattern strongly indicate that the graphene/MgO interface is commensurate and involves both an interfacial reconstruction and chemical reactions. Since the O–O nearest-neighbor distance in bulk-terminated MgO(111) is about 2.8 Å,⁹² an incommensurate graphene/oxide interface will result if the oxide surface does not reconstruct. Carbon A sites and B sites would thus experience an ensemble of different substrate environments, resulting in the same average environment at both A and B sites. Instead, the 3-fold symmetry observed for single and few-layer films,³¹ coincident with the formation of an oxidized carbon peak carbon 1s X-ray photoemission peak strongly suggests significant carbon and/or oxide reconstruction at the interface.^{30,32} Indeed, this first layer may not be pure “graphene”, but a partially oxidized, albeit ordered, form.

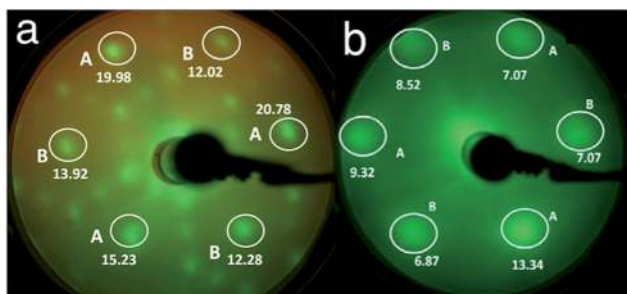


Fig. 3 The low energy electron diffraction (LEED) pattern of 1 ML graphene on MgO exhibits C_{3v} symmetry, as illustrated in (a) where the background-subtracted intensities (arbitrary units) for ‘A’ and ‘B’ spots (circled) have an average intensity of 18.7 ± 3, and 12.9 ± 1 respectively. The uncertainties are the standard deviations. Other spots in the image are weaker and are attributed to multiple diffraction. The LEED pattern was acquired at 80 eV beam energy. (b) The intensity analysis of the average background-subtracted intensity (arbitrary units) LEED pattern (75 eV beam energy) of graphene film, 2.5 ML thick on MgO has the ‘A’ sites is 9.9 (±3), and that of the B sites is 7.5 (±0.9). From ref. 29 and 32.

A band gap is evident in the combined photoemission and inverse photoemission,^{28,30,31} as seen in Fig. 2, for graphene on MgO(111), and although heavily p-doped by the oxide interface, this graphene is insulating. Charge transport data^{30,32} for a single layer C(111) film (produced by PVD) on MgO(111) are also shown in Fig. 4. Fig. 5 shows a logarithmic plot of the resistance as a function of reciprocal temperature, which is linear and exhibits the negative magnetoresistance characteristic of a nonmetal. The transport data yield a carrier-hopping activation energy of 0.64 (±0.05) eV,^{30,32} consistent with a band gap of 0.5 eV or greater that is estimated from the combined photoemission/inverse photoemission.^{31,32} Given that this picture is also evident in model calculations for single layer graphene between boron nitride layers,²³ graphene on BN,^{25,27} SiO₂,²⁴ Al₂O₃(0001) (ref. 35) and MgO,³⁴ and the possibly controversial^{53,54,91} experimental band gap for graphene on SiC,^{28,40} charge disorder or breaking of the A and B site symmetry matters.

Other oxides should be considered in the future, but identifying a suitable surface where there is an interface lattice match with graphene, as in the case of MgO(111), is a challenge. For graphene grown on Co₃O₄(111), there is no evidence of a band gap, and extensive p-doping of the graphene is likely.^{32,93} Chromia, *i.e.* Cr₂O₃, has potential to be more effective than MgO(111) if the interface is stable and suitably terminated. The

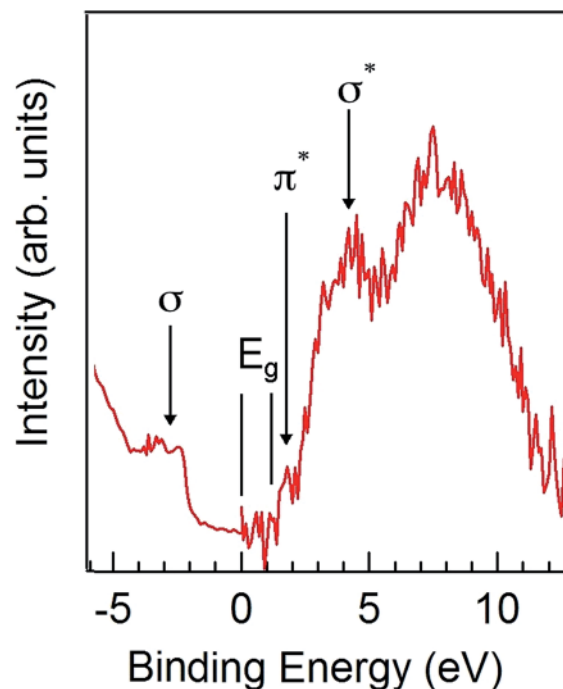


Fig. 4 Angle-integrated valence band ultraviolet photoemission (UPS) (left) and k-vector resolved inverse photoelectron (right) spectroscopy data for a graphene film on MgO(111). The photoemission data correspond closely to spectra of graphene on transition metal substrates, but the data here indicate a band gap E_g of ~0.5 eV. There is considerable uncertainty in the value of E_g due to the limited resolution of the inverse photoemission, as well as final state effects in both spectra. Binding energies are referenced to the Fermi level as E – E_F. The π*, π, σ*, and σ weighted features indicated. Adapted from ref. 31.

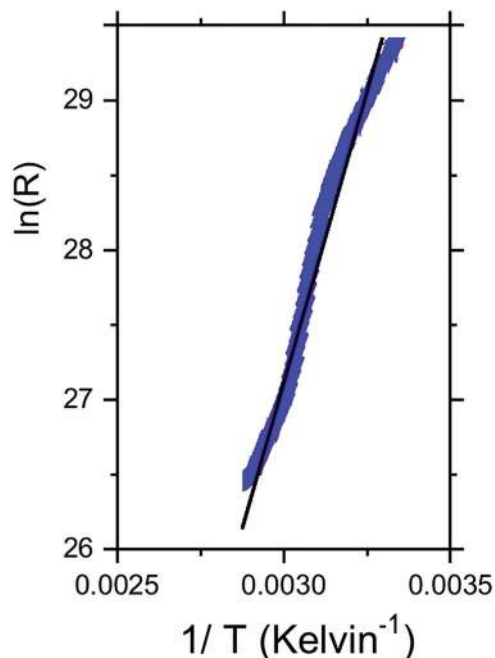


Fig. 5 Plot of $\ln(\text{resistance})$ versus reciprocal temperature for single layer of C(111) on MgO(111). Data shows semiconducting behavior with a charge carrier hopping activation energy of ~ 0.6 eV. Blue: data; black line: least squares fit. Adapted from ref. 32.

attraction with chromia^{94,95} is the voltage controlled high surface polarization.^{96–98} Both the graphene $\text{Co}_3\text{O}_4(111)$ and $\text{Cr}_2\text{O}_3(001)$ to graphene interfaces are incommensurate, that is say that while graphene is aligned with the substrate when grown directly on $\text{Co}_3\text{O}_4(111)$, the graphene lattice period is not identical with the substrate, at the interface. This makes symmetry reduction through different the chemical interactions at the graphene A and B sites more complex, if not more difficult. $\text{Cr}_2\text{O}_3(001)$ is also attractive as having a less polar surface than MgO(111), thus less likely to p-dope the adjacent graphene layer extensively. As emphasized by Ballhausen,⁹⁹ electrostatic crystal-field and quantum-mechanical ligand-field theories are equivalent as far as symmetry (and symmetry breaking) are concerned. The reason for MgO being an ideal substrate is the six-fold symmetry of the NaCl-type (111) plane in combination with interface (not bulk) lattice parameters that ensure epitaxial growth and a virtually complete AB splitting.

D. Band-gap formation in graphene through sublattice modification

The reduction of symmetry, by breaking the chemical equivalency of the graphene A and B sites, leads to a reduction in symmetry from C_{6v} point group to the C_{3v} point group. In the C_{3v} point group, away from $\bar{\Gamma}$ the center of the Brillouin zone, there is no mirror plane symmetry in the Brillouin zone line to K , the edge of the graphene Brillouin zone, about which the Dirac cone is centered. With the loss of mirror plane symmetry at K , the π band may not retain pure p_z character, particularly if the

graphene does not remain flat in the x - y plane as a result of the symmetry reduction. It should be recognized, as throughout surface science, there is an interplay between the energy cost or strain energy for a surface (and in this case graphene) structural reconstructions and reduction in energy opening up a band gap. More importantly, when a reduction of the symmetry is allowed, graphene can lower the total free energy of the system and a band gap will open at the Dirac point.

To explain how symmetry breaking substrates affect the band structure of graphene, we have modeled the substrate as a crystal-field source and treated the graphene as a tight-binding p_z -electron system. As emphasized by Ballhausen⁹⁹ as well as others,⁴¹ crystal-field and chemical effects are equivalent as far as symmetry-breaking is concerned, and the difference between the present theory and a more complete description of the electronic structure is the same as between Bethe-level crystal-field theory and ligand-field theory. For the theoretical background and the tight-binding calculation, see ref. 4, 41 and 100 and references therein.

Fig. 6 shows the considered structure, distinguishing between the two sublattices in graphene. The bright (A) and dark (B) atoms sit on top of crystallographically nonequivalent sites of the substrate, so that the orbital or “on-site” energies of the p_z electrons are different. Ignoring a physically unimportant zero-point energy, the on-site energies for the A and B atoms are $E_{A/B} = \pm V_{CF}/2$. Here the crystal-field parameter V_{CF} increases with decreasing distance between graphene layer and substrate. The corresponding tight-binding Hamiltonian is

$$\mathcal{H} = \begin{pmatrix} +V_{CF}/2 & T \\ T^* & -V_{CF}/2 \end{pmatrix} \quad (1)$$

where $T = t \sum_B \exp(i\mathbf{k} \cdot \mathbf{R}_{AB})$ describes the interatomic hopping between the A and B sites:

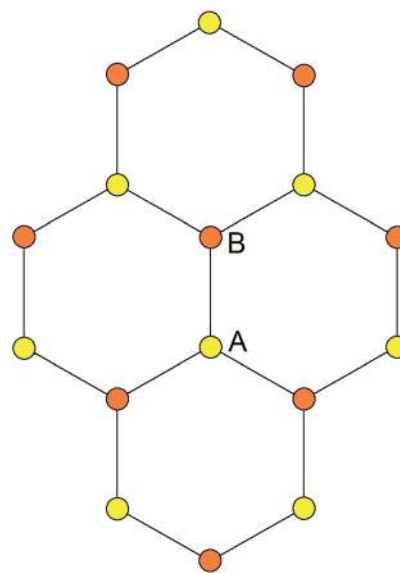


Fig. 6 Atomic structure of graphene. A-site atoms have B-site nearest neighbors only, and vice versa. In the present context, A (yellow) and B (red) atoms corresponds to different substrate positions.

$$T = t(\exp(ik_y a) + 2 \exp(-ik_y a/2) \cos(\sqrt{3}k_x a/2)) \quad (2)$$

The appearance of T^* in the bottom left corner of the Hamiltonian of eqn (1) is mandated by hermiticity, but it can also be interpreted in terms of interchanged sublattices ($\mathbf{R}_{AB} = -\mathbf{R}_{BA}$).

The solution of eqn (1) is trivial and yields two energy branches

$$E_{\pm}(\mathbf{k}) = \pm \sqrt{V_{CF}^2/4 + T^*(\mathbf{k})T(\mathbf{k})} \quad (3)$$

where V_{CF} can be shown to equal the band gap. This is evident from Fig. 7, which compares the familiar “spider legs” of the graphene Brillouin-zone boundary dispersion relation $E_i(\mathbf{k})$ without (a) and with (b) symmetry breaking. For $V_{CF} = 0$, the legs have needle-shaped feet which touch the Dirac points (dots), indicating linear dispersion near the Dirac point and zero effective mass. In the presence of the symmetry-breaking potential $\pm V_{CF}/2$, a gap of width V_{CF} opens and the ends of the legs become curved, corresponding to a non-zero effective mass.

Near any of the Dirac points (K_x, K_y), the energy can be expanded in terms of the small wave-vector difference $\mathbf{q} = (k_x - K_x, k_y - K_y)$. This leads to $T^*T = 3a^2q^2t^2/4$ where $q = (q_x^2 + q_y^2)^{1/2}$, and the corresponding dispersion relation, $E_{\pm} = V_{CF}/2 + 3a^2q^2t^2/4V_{CF}$, yields the effective mass $m^* = 2\hbar^2V_{CF}/3a^2$. Since the lattice parameter a does not vary very much from system to system, the effective mass is essentially determined by the band gap V_{CF} . It is convenient to consider the ratio $m^*/m = 4V_{CF}E_H a_0^2/3t^2 a^2$, where m is the electron mass, $E_H = 13.6$ eV, and $a_0 = 0.529$ Å. Taking $V_{CF} = 0.5$ eV, $t = 2.7$ eV, and $a = 2.46$ Å yields $m^*/m = 0.058$, which can be regarded as a typical value for the effective mass. This is a smaller effective mass than is the case when the band gap is opened by uniaxial strain.⁴

Note that the gap is the same for all Dirac points (Fig. 8), that is, all spider legs have the same length. The difference between the A and B sites appears in the wave functions $\psi_{\pm}(\mathbf{r})$ corresponding to the two energy branches of eqn (3): at the Dirac points, the wave functions are entirely of the A type (ψ_+) or of the B type (ψ_-). For example, n-doping means that only A sites are occupied. In the absence of currents in the graphene sheet, the

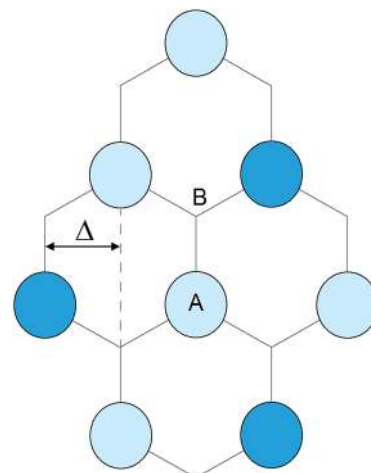


Fig. 8 Schematic real-space electron density (top view of p_z electrons) for n-doped graphene and positive V_{CF} .

wave functions must be real. At the Dirac points, this can be achieved by superposing solutions for \mathbf{K} and $-\mathbf{K}$, exploiting that $\exp(i\mathbf{K}\cdot\mathbf{R}_A) + \exp(-i\mathbf{K}\cdot\mathbf{R}_A) = 2 \cos(\mathbf{K}\cdot\mathbf{R}_A)$. Fig. 8 shows typical p_z electron density that might be possible for graphene, as induced by the substrate. For n-doped graphene and positive V_{CF} , the extra electrons occupies the A sites, and the electron density of the dark blue atoms is 4 times higher than that of the bright blue atoms. For p-doped graphene, the same argument would of course apply to hole carriers.

For the derivation and interpretation of Fig. 8, it is convenient to use $\mathbf{K} = (4\pi/3\sqrt{3}a, 0)$. The horizontal distance between columns of atoms, $\Delta = \sqrt{3}a/2$, then corresponds to a phase

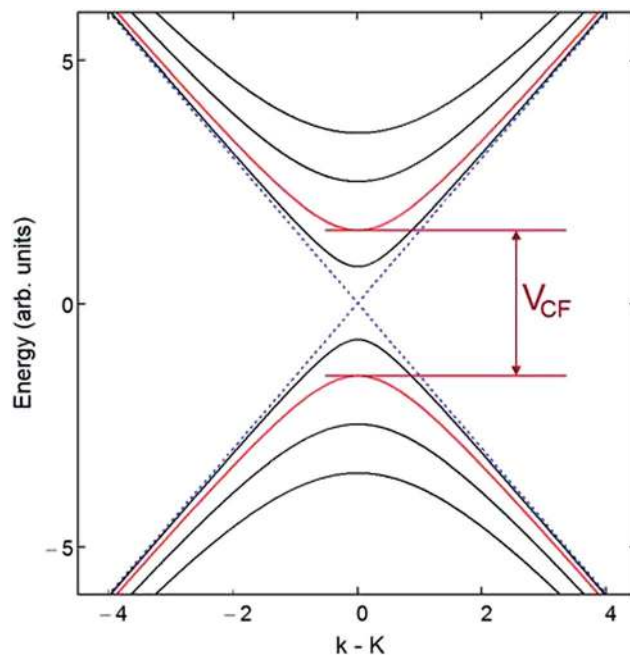


Fig. 9 The relationship of the band gap near the Dirac point and the relative on-site energies of the A and B sites by $\pm V_{CF}/2$.

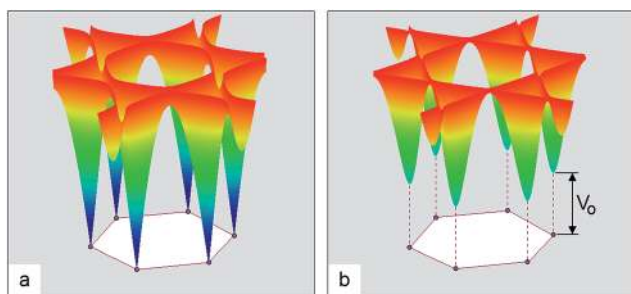


Fig. 7 The energy dispersion $E_+(k_x, k_y)$ for (a) perfect graphene ($V_{CF} = 0$) and (b) graphene on a symmetry-breaking substrate ($V_{CF} = 2V_0 = 0.8t$).

shift of $2\pi/3 = 120^\circ$. This means a shift by 3Δ or 360° reproduces the original charge density. It should be noted that opening the band gap does result in an increase in carrier effective mass, and the greater the band gap, the greater the effective mass, as summarized in Fig. 9.

E. Conclusions

Band gap engineering of graphene is certainly possible, and this opens up the possibility of devices in very strict 2 dimensional conduction channels, but at the cost of increased effective mass. Effective mobilities for graphene on MgO have not been reported, but for graphene without a band gap (or at least a very nearly negligible band gap), transferred to various substrates, room temperature mobilities above $\sim 20\,000\text{ cm}^2\text{ V}^{-1}\text{ s}^{-1}$ (ref. 62, 63 and 101) are possible, but more often below $3000\text{ cm}^2\text{ V}^{-1}\text{ s}^{-1}$ are reported.^{52,102,103} While such mobility limitations are for the most part due to factors other than band structure,^{41,52,53,57,58,103} the introduction of a band gap can only further decrease carrier mobilities (Fig. 8 and 9).

It is important to realize that extrinsic mechanisms like adsorbate or substrate interactions may also dope the graphene. If the advantages accrued by converting graphene from a gapless semiconductor to a band gap semiconductor, it is important that the graphene then not be over-doped to imitate a degeneratively doped semiconductor. We note that there are flaws in estimating the band gap in graphene with density-functional theory (DFT): on the one hand, DFT is notorious for underestimating band gaps due to correlations, but on the other hand, wave-vector sampling techniques might not sample the density of states with a fine enough wave-vector grid and therefore overestimate a band gap. While correlation effects in graphene are debatable, our present approach explains band-gap openings in graphene with very high k -space accuracy.

Acknowledgements

This work was supported by the Semiconductor Research Corporation under tasks 2123.001 and 2358.001, and by C-SPIN, part of STARnet, a Semiconductor Research Corporation program sponsored by MARCO and DARPA (SRC 2381.002 and 2381.003). Further support was provided through the National Science Foundation funded Nebraska MRSEC DMR-0820521, the Army Research Office W911NF-10-2-0099, and the Nebraska Center for Materials and Nanoscience.

Notes and references

- V. M. Pereira, A. H. C. Neto and N. M. R. Peres, *Phys. Rev. B: Condens. Matter Mater. Phys.*, 2009, **80**, 045401.
- G. Gui, J. Li and J. Zhong, *Phys. Rev. B: Condens. Matter Mater. Phys.*, 2008, **78**, 075435.
- I. I. Naumov and A. M. Bratkovsky, *Phys. Rev. B: Condens. Matter Mater. Phys.*, 2011, **84**, 245444.
- P. Kumar, R. Skomski, P. Manchanda, A. Kashyap and P. A. Dowben, *Curr. Appl. Phys.*, 2014, **14**, S136–S139.
- Y. W. Son, M. L. Cohen and S. G. Louie, *Phys. Rev. Lett.*, 2006, **97**, 216803.
- V. Barone, O. Hod and G. E. Scuseria, *Nano Lett.*, 2006, **6**, 2748–2754.
- D. Prezzi, D. Varsano, A. Ruini, A. Marini and E. Molinari, *Phys. Rev. B: Condens. Matter Mater. Phys.*, 2008, **77**, 041404.
- L. Yang, M. L. Cohen and S. G. Louie, *Nano Lett.*, 2007, **7**, 3112–3115.
- L. Yang, C. H. Park, Y. W. Son, M. L. Cohen and S. G. Louie, *Phys. Rev. Lett.*, 2007, **99**, 186801.
- D. Prezzi, D. Varsano, A. Ruini and E. Molinari, *Phys. Rev. B: Condens. Matter Mater. Phys.*, 2011, **84**, 041401.
- M. Y. Han, B. Özyilmaz, Y. Zhang and P. Kim, *Phys. Rev. Lett.*, 2007, **98**, 206805.
- X. Li, X. Wang, L. Zhang, S. Lee and H. Dai, *Science*, 2008, **319**, 1229–1232.
- S. Linden, D. Zhong, A. Timmer, N. Aghdassi, J. H. Franke, H. Zhang, X. Feng, K. Müllen, H. Fuchs, L. Chi and H. Zacharias, *Phys. Rev. Lett.*, 2012, **108**, 216801.
- T. H. Vo, M. Shekhirev, D. A. Kunkel, M. D. Morton, E. Berglund, L. Kong, P. M. Wilson, P. A. Dowben, A. Enders and A. Sinitskii, *Nat. Commun.*, 2014, **5**, 3189.
- K. Nakada, M. Fujita, G. Dresselhaus and M. S. Dresselhaus, *Phys. Rev. B: Condens. Matter Mater. Phys.*, 1996, **54**, 17954.
- K. Wakabayashi, M. Fujita, H. Ajiki and M. Sigrist, *Phys. Rev. B: Condens. Matter Mater. Phys.*, 1999, **59**, 8271.
- P. Sessi, J. R. Guest, M. Bode and N. P. Guisinger, *Nano Lett.*, 2009, **9**, 4343–4347.
- R. Balog, B. Jørgensen, L. Nilsson, M. Andersen, E. Rienks, M. Bianchi, M. Fanetti, E. Lægsgaard, A. Baraldi, S. Lizzit, Z. Sljivancanin, F. Besenbacher, B. Hammer, T. G. Pedersen, P. Hofmann and L. Hornekær, *Nat. Mater.*, 2010, **9**, 315–319.
- D. W. Boukhvalov and M. I. Katsnelson, *J. Phys.: Condens. Matter*, 2009, **21**, 344205.
- J. Berashevich and T. Chakraborty, *Phys. Rev. B: Condens. Matter Mater. Phys.*, 2009, **80**, 033404.
- S. Niyogi, E. Bekyarova, M. E. Itkiss, H. Zhang, K. Shepperd, J. Hicks, M. Sprinkle, C. Berger, C. N. Lau, W. A. deHeer, E. H. Conrad and R. C. Haddon, *Nano Lett.*, 2010, **10**, 4061–4066.
- J. Sławińska, I. Zasada, P. Kosiński and Z. Klusek, *Phys. Rev. B: Condens. Matter Mater. Phys.*, 2010, **82**, 085431.
- R. Quhe, J. Zheng, G. Luo, Q. Liu, R. Qin, J. Zhou, D. Yu, S. Nagase, W.-N. Mei, Z. Gao and J. Lu, *NPG Asia Mater.*, 2012, **4**, e6.
- P. Shemella and S. K. Nayak, *Appl. Phys. Lett.*, 2009, **94**, 032101.
- G. Giovannetti, P. A. Khomyakov, G. Brocks, P. J. Kelly and J. van den Brink, *Phys. Rev. B: Condens. Matter Mater. Phys.*, 2007, **76**, 073103.
- B. Hunt, J. D. Sanchez-Yamagishi, A. F. Young, M. Yankowitz, B. J. LeRoy, K. Watanabe, T. Taniguchi, P. Moon, M. Koshino, P. Jarillo-Herrero and R. C. Ashoori, *Science*, 2013, **340**, 1427–1430.
- M. Kindermann, B. Uchoa and D. L. Miller, *Phys. Rev. B: Condens. Matter Mater. Phys.*, 2012, **86**, 115415.

- 28 S. Y. Zhou, G.-H. Gweon, A. V. Fedorov, P. N. First, W. A. de Heer, D.-H. Lee, F. Guinea, A. H. C. Neto and A. Lanzara, *Nat. Mater.*, 2007, **6**, 770–775.
- 29 S. Gaddam, C. Bjelkevig, S. Ge, K. Fukutani, P. A. Dowben and J. A. Kelber, *J. Phys.: Condens. Matter*, 2011, **23**, 072204.
- 30 J. A. Kelber, S. Gaddam, C. Vamala, S. Eswaran and P. A. Dowben, *Proc. SPIE*, 2011, **8100**, 81000Y.
- 31 L. Kong, C. Bjelkevig, S. Gaddam, M. Zhou, Y. H. Lee, G. H. Han, H. K. Jeong, N. Wu, Z. Zhang, J. Xiao, P. A. Dowben and J. A. Kelber, *J. Phys. Chem. C*, 2010, **114**, 21618–21624.
- 32 J. A. Kelber, M. Zhou, S. Gaddam, F. L. Pasquale, L. M. Kong and P. A. Dowben, *ECS Trans.*, 2012, **45**, 49–61.
- 33 K.-A. Min, J. Park, J. Ryou, S. Hong and A. Soon, *Curr. Appl. Phys.*, 2013, **13**, 803–807.
- 34 S. B. Cho and Y.-C. Chung, *J. Mater. Chem. C*, 2013, **1**, 1595–1600.
- 35 B. Huang, Q. Xu and S.-H. Wei, *Phys. Rev. B: Condens. Matter Mater. Phys.*, 2011, **84**, 155406.
- 36 E. McCann, *Phys. Rev. B: Condens. Matter Mater. Phys.*, 2006, **74**, 161403.
- 37 H. Min, B. Sahu, S. K. Banerjee and A. H. MacDonald, *Phys. Rev. B: Condens. Matter Mater. Phys.*, 2007, **75**, 155115.
- 38 K. F. Mak, C. H. Lui, J. Shan and T. F. Heinz, *Phys. Rev. Lett.*, 2009, **102**, 256405.
- 39 Y. Zhang, T.-T. Tang, C. Girit, Z. Hao, M. C. Martin, A. Zettl, M. F. Crommie, Y. R. Shen and F. Wang, *Nature*, 2009, **459**, 820–823.
- 40 S. Y. Zhou, D. A. Siegel, A. V. Fedorov, F. El Gabaly, A. K. Schmid, A. H. Castro Neto, D.-H. Lee and A. Lanzara, *Nat. Mater.*, 2008, **7**, 259–260.
- 41 A. Bostwick, T. Ohta, J. L. McChesney, K. V. Emtsev, T. Seyller, K. Horn and E. Rotenberg, *New J. Phys.*, 2007, **9**, 385.
- 42 G. Cocco, E. Cadelano and L. Colombo, *Phys. Rev. B: Condens. Matter Mater. Phys.*, 2010, **81**, 241412.
- 43 S.-M. Choi, S.-H. Jhi and Y.-W. Son, *Phys. Rev. B: Condens. Matter Mater. Phys.*, 2010, **81**, 081407.
- 44 Z. H. Ni, T. Yu, Y. H. Lu, Y. Y. Wang, Y. P. Feng and Z. X. Shen, *ACS Nano*, 2008, **2**, 2301–2305.
- 45 K. S. Kim, Y. Zhao, H. Jang, S. Y. Lee, J. M. Kim, K. S. Kim, J.-H. Ahn, P. Kim, J.-Y. Choi and B. H. Hong, *Nature*, 2009, **457**, 706–710.
- 46 Z. H. Ni, H. M. Wang, Y. Ma, J. Kasim, Y. H. Wu and Z. X. Shen, *ACS Nano*, 2008, **2**, 1033–1039.
- 47 J. Hicks, A. Tejada, A. Taleb-Ibrahimi, M. S. Nevius, F. Wang, K. Shepperd, J. Palmer, F. Bertran, P. Le Fèvre, J. Kunc, W. A. de Heer, C. Berger and E. H. Conrad, *Nat. Phys.*, 2013, **9**, 49–54.
- 48 Z. H. Chen, Y. M. Lin, M. J. Rooks and P. Avouris, *Phys. E*, 2007, **40**, 228–232.
- 49 X. R. Wang, Y. Ouyang, L. Jiao, H. Wang, L. Xie, J. Wu, J. Guo and H. Dai, *Nat. Nanotechnol.*, 2011, **6**, 563–567.
- 50 Y. M. Lin, V. Perebeinos, Z. H. Chen and P. Avouris, *Phys. Rev. B: Condens. Matter Mater. Phys.*, 2008, **78**, 161409(R).
- 51 K. Todd, H. T. Chou, S. Amasha and D. Goldhaber-Gordon, *Nano Lett.*, 2009, **9**, 416–421.
- 52 J. Baringhaus, M. Ruan, F. Edler, A. Tejada, M. Sicot, A. Taleb-Ibrahimi, A.-P. Li, Z. Jiang, E. H. Conrad, B. Berger, C. Tegenkamp and W. A. de Heer, *Nature*, 2014, **506**, 349.
- 53 E. Rotenberg, A. Bostwick, T. Ohta, J. L. McChesney, T. Seyller and K. Horn, *Nat. Mater.*, 2008, **7**, 258–259.
- 54 T. Ohta, A. Bostwick, J. L. McChesney, T. Seyller, K. Horn and E. Rotenberg, *Phys. Rev. Lett.*, 2007, **98**, 206802.
- 55 F. Varchon, R. Feng, J. Hass, X. Li, B. Ngoc Nguyen, C. Naud, P. Mallet, J.-Y. Veuillen, C. Berger, E. H. Conrad and L. Magaud, *Phys. Rev. Lett.*, 2007, **99**, 126805.
- 56 V. W. Brar, Y. Zhang, Y. Yayon, T. Ohta, J. L. McChesney, A. Bostwick, E. Rotenberg, K. Horn and M. F. Crommie, *Appl. Phys. Lett.*, 2007, **91**, 122102.
- 57 E. H. Hwang and S. Das Sarma, *Phys. Rev. B: Condens. Matter Mater. Phys.*, 2007, **75**, 205418.
- 58 A. Bostwick, T. Ohta, T. Seyller, K. Horn and E. Rotenberg, *Nat. Phys.*, 2007, **3**, 36–40.
- 59 Y. Qi, S. H. Rhim, G. F. Sun, M. Weinert and L. Li, *Phys. Rev. Lett.*, 2010, **105**, 085502.
- 60 M. A. Fanton, J. A. Robinson, C. Puls, Y. Liu, M. J. Hollander, B. E. Weiland, M. LaBella, K. Trumbull, R. Kasarda, C. Howsare, J. Stitt and D. W. Snyder, *ACS Nano*, 2011, **5**, 8062–8069.
- 61 A. H. C. Neto, F. Guinea, N. M. R. Peres, K. S. Novoselov and A. K. Geim, *Rev. Mod. Phys.*, 2009, **81**, 109.
- 62 C. R. Dean, A. F. Young, I. Meric, C. Lee, L. Wang, S. Sorgenfrei, K. Watanabe, T. Taniguchi, P. Kim, K. L. Shepard and J. Hone, *Nat. Nanotechnol.*, 2010, **5**, 722–726.
- 63 W. Gannett, W. Regan, K. Watanabe, T. Taniguchi, M. F. Crommie and A. Zettl, *Appl. Phys. Lett.*, 2011, **98**, 242105.
- 64 N. Petrone, C. R. Dean, I. Meric, A. M. van der Zande, P. Y. Huang, L. Wang, D. Muller, K. L. Shepard and J. Hone, *Nano Lett.*, 2012, **12**, 2751–2756.
- 65 C. Bjelkevig, Z. Mi, J. Xiao, P. A. Dowben, L. Wang, W.-N. Mei and J. A. Kelber, *J. Phys.: Condens. Matter*, 2010, **22**, 302002.
- 66 C. Oshima, A. Itoh, E. Rokuta, T. Tanaka, K. Yamashita and T. Sakurai, *Solid State Commun.*, 2000, **116**, 37–40.
- 67 T. Brugger, S. Günther, B. Wang, J. H. Dil, M.-L. Bocquet, J. Osterwalder, J. Winterlin and T. Greber, *Phys. Rev. B: Condens. Matter Mater. Phys.*, 2009, **79**, 045407.
- 68 A. B. Preobrajenski, A. S. Vinogradov and N. Mårtensson, *Surf. Sci.*, 2005, **582**, 21–30.
- 69 A. Goriachko, Y. B. He and H. Over, *J. Phys. Chem. C*, 2008, **112**, 8147–8152.
- 70 M. L. Ng, A. B. Preobrajenski, A. S. Vinogradov and N. Mårtensson, *Surf. Sci.*, 2008, **602**, 1250–1255.
- 71 A. Goriachko, Yunbin, M. Knapp and H. Over, *Langmuir*, 2007, **23**, 2928–2931.
- 72 M. Morscher, M. Corso, T. Greber and J. Osterwalder, *Surf. Sci.*, 2006, **600**, 3280–3284.
- 73 W. Auwärter, T. J. Kreuzt, T. Greber, J. Osterwalder, M. Corso, T. Brugger, S. Berner, J. Osterwalder and T. Greber, *Surf. Sci.*, 1999, **429**, 229–236.

- 74 M. Muntwiler, M. Hengsberger, A. Dolocan, H. Neff, T. Greber and J. Osterwalder, *Phys. Rev. B: Condens. Matter Mater. Phys.*, 2007, **75**, 075407.
- 75 M. Muntwiler, W. Auwärter, F. Baumberger, M. Hoesch, T. Greber and J. Osterwalder, *Surf. Sci.*, 2001, **472**, 125–132.
- 76 Y. Gamou, M. Terai, A. Nagashima and C. Oshima, *Sci. Rep. Res. Inst., Tohoku Univ., Ser. A*, 1997, **44**, 211.
- 77 A. Nagashima, N. Tejima, Y. Gamou, T. Kawai and C. Oshima, *Phys. Rev. Lett.*, 1995, **75**, 3918.
- 78 A. Nagashima, N. Tejima, Y. Gamou, T. Kawai and C. Oshima, *Phys. Rev. B: Condens. Matter Mater. Phys.*, 1995, **51**, 4606.
- 79 K. Zumbärgel, K. Wulff, C. Eibl, M. Donath and M. Hengsberger, *Phys. Rev. B: Condens. Matter Mater. Phys.*, 2008, **78**, 085422.
- 80 T. Lin, Y. Wang, H. Bi, D. Wan, F. Huang, X. Xie and M. Jiang, *J. Mater. Chem.*, 2012, **22**, 2859–2862.
- 81 X. Ding, G. Ding, X. Xie, F. Huang and M. Jiang, *Carbon*, 2011, **49**, 2522–2525.
- 82 J. A. Kelber, Direct Graphene Growth on Dielectric Substrates, *Graphene, Carbon Nanotubes and Nanostructures: Techniques and Applications*, CRC Press, 2013, ch. 5, pp. 89–113.
- 83 M. Yankowitz, J. Xue, D. Cormode, J. D. Sanchez-Yamagishi, K. Watanabe, T. Taniguchi, P. Jarillo-Herrero, P. Jacquod and B. J. LeRoy, *Nat. Phys.*, 2012, **8**, 382–386.
- 84 C. H. Park, L. Yang, Y.-W. Son, M. L. Cohen and S. G. Louie, *Nat. Phys.*, 2008, **4**, 213–217.
- 85 C. H. Park, L. Yang, Y.-W. Son, M. L. Cohen and S. G. Louie, *Phys. Rev. Lett.*, 2008, **101**, 126804.
- 86 L. Brey and H. A. Fertig, *Phys. Rev. Lett.*, 2009, **103**, 046809.
- 87 P. Bursset, A. Yeyati, L. Brey and H. Fertig, *Phys. Rev. B: Condens. Matter Mater. Phys.*, 2011, **83**, 195434.
- 88 R. V. Gorbachev, A. K. Geim, M. I. Katsnelson, K. S. Novoselov, T. Tudorovskiy, I. V. Grigorieva, A. H. MacDonald, S. V. Morozov, K. Watanabe, T. Taniguchi and L. A. Ponomarenko, *Nat. Phys.*, 2012, **8**, 896–901.
- 89 Y. Li, P. Chen, G. Zhou, J. Li, J. Wu, B.-L. Gu, S. B. Zhang and W. Duan, *Phys. Rev. Lett.*, 2012, **109**, 206802.
- 90 J. Zhou, L. Wang, R. Qin, J. Zheng, W.-N. Mei, P. Dowben, S. Nagase, Z. Gao and J. Lu, *J. Phys. Chem. C*, 2011, **115**, 25273–25280.
- 91 T. Ohta, A. Bostwick, J. L. McChesney, T. Seyller, K. Horn and E. Rotenberg, *Phys. Rev. Lett.*, 2007, **98**, 206802.
- 92 V. K. Lazarov, R. Plass, H.-C. Poon, D. K. Saldin, M. Weinert, S. A. Chambers and M. Gajdardziska-Josifovska, *Phys. Rev. B: Condens. Matter Mater. Phys.*, 2005, **71**, 115434.
- 93 M. Zhou, F. L. Pasquale, P. A. Dowben, A. Boosalis, M. Schubert, V. Darakchieva, R. Yakimova, L. Kong and J. A. Kelber, *J. Phys.: Condens.*, 2012, **24**, 072201.
- 94 X. Chen, H. Kazi, Y. Cao, B. Dong, F. L. Pasquale, J. A. Colón Santana, S. Cao, R. Welch, Ch. Binek, A. Enders, J. A. Kelber and P. A. Dowben, *Mater. Chem. Phys.*, submitted.
- 95 S. Stuart, E. Sachet, J. P. Maria, J. E. Rowe, M. C. Ulrich and D. Dougherty, <http://meetings.aps.org/link/BAPS.2014.MAR.F6.5>, Bulletin of the American Physical Society, 2014, F6.5.
- 96 X. He, Y. Wang, N. Wu, A. N. Caruso, E. Vescovo, K. D. Belashchenko, P. A. Dowben and Ch. Binek, *Nat. Mater.*, 2010, **9**, 579–585.
- 97 N. Wu, X. He, A. Wysocki, U. Lanke, T. Komesu, K. D. Belashchenko, Ch. Binek and P. A. Dowben, *Phys. Rev. Lett.*, 2011, **106**, 087202.
- 98 S. Cao, X. Zhang, N. Wu, A. T. N'Diaye, G. Chen, A. K. Schmid, X. Chen, W. Echtenkamp, A. Enders, Ch. Binek and P. A. Dowben, *New J. Phys.*, 2014, **16**, 073021.
- 99 C. J. Ballhausen, *Ligand Field Theory*, McGraw-Hill, New York, 1962.
- 100 S. Reich, J. Maultzsch, C. Thomsen and P. Ordejn, *Phys. Rev. B: Condens. Matter Mater. Phys.*, 2002, **66**, 035412.
- 101 S. Kim, J. Nah, I. Jo, D. Shahrjerdi, L. Colombo, Z. Yao, E. Tutuc and S. K. Banerjee, *Appl. Phys. Lett.*, 2009, **94**, 062107.
- 102 H. Lv, H. Wu, K. Xiao, W. Zhu, H. Xu, Z. Zhang and H. Qian, *Appl. Phys. Lett.*, 2013, **102**, 183107.
- 103 D. K. Ferry, *J. Comput. Electron.*, 2013, **12**, 76–84.